



# Comparative study of six failure criteria via numerical simulation of stamped DP600 steel

Lucas Marcondes Ribas<sup>1</sup> · Manolo Lutero Gipiela<sup>1</sup> · Sérgio Fernando Lajarin<sup>1</sup> · Ravilson Antonio Chemin Filho<sup>1</sup> · Paulo Victor Prestes Marcondes<sup>1</sup>

Received: 19 January 2022 / Accepted: 25 May 2022

© The Author(s), under exclusive licence to Springer-Verlag London Ltd., part of Springer Nature 2022

## Abstract

During the development of an automobile part obtained by stamping process, time and money are required aiming process planning and setup of a new tooling. One of the difficulties in stamping is to know if the chosen material will have sufficient formability to reach the final form required by the project. Because of this difficulty, it is very interesting to propose a method that can accurately simulate the forming process. The failure criteria can be mathematical or empirical models capable of determining the onset of necking for each stress/strain states. It is interesting to find a failure criterion that can be easily determined and provides a good ability to detect the failure accurately. In this study, six different failure criteria were studied. Five of them are classified as ductile damage models and they depend on the stress triaxiality and plastic strain. The last criterion depends only on the deformations in the main directions and it is called the forming limit curve (FLC). Computational models through finite element analysis (FEA) were used. The formability was evaluated by monitoring the displacement of the punch until the failure of the material. Lou and Huh criterion and Johnson-Cook criterion have been able to provide approximation errors in the range of 0.7–5% which makes them interesting for practical implementation in the industry.

**Keywords** Stamping · Failure criteria · AHSS · Finite element analysis

## 1 Introduction

The significant increase of advanced high strength steels (AHSS) applications in vehicles was necessary due to the environmental demands that lead to decreased pollutants by reducing vehicle weights and maintaining the mechanical

strength levels of materials already used in industry [1]. During the design phase of a product, time and money are spent during the tooling setup [2]. Depending on the geometry of the desired product, the selected material can be unable to deform to achieve such requirement. Determining a failure criterion that can accurately describe the fracture mechanism of a metallic material can be very useful in sheet metal part development.

Two groups of failure criteria modes that are applied in the stamping process were carried out. The first is the forming limit curve (FLC) and the second is the ductile damage mode criteria. The FLC criterion is usually obtained by Nakazima test based on the two main strains, width-by-length. On the other hand, the ductile damage criteria are based on the complete state of stresses and strains involved in the stamping process [3]. The fracture starts when the equivalent plastic strain reaches a critical value  $D_c$ , Eq. (1).

$$D(\bar{\epsilon}_p) = \int_0^{\bar{\epsilon}_f} \frac{d\bar{\epsilon}_p}{f(\eta, \bar{\theta})} \quad (1)$$

---

This article is part of Topical Collection on *New Intelligent Manufacturing Technologies through the Integration of Industry 4.0 and Advanced Manufacturing*

✉ Manolo Lutero Gipiela  
mgipiela@yahoo.com.br

Lucas Marcondes Ribas  
lmarcondesribas21@gmail.com

Sérgio Fernando Lajarin  
espanhol@ufpr.br

Ravilson Antonio Chemin Filho  
ravilson@ufpr.br

Paulo Victor Prestes Marcondes  
marcondes@ufpr.br

<sup>1</sup> Federal University of Paraná, Curitiba, Brazil

In Eq. (1),  $\bar{\epsilon}_p$  is the equivalent plastic strain,  $\bar{\epsilon}_f$  is the equivalent plastic strain for fracture, and  $D(\bar{\epsilon}_p)$  is called the ductile failure criteria or damage factor, which indicates the onset of fracture when it reaches the critical value  $D_c = 1$ , since at the time of fracture the relation  $\bar{\epsilon}_p = \bar{\epsilon}_f$  is suggested by [4]. The parameters  $\eta$  and  $\bar{\theta}$  are called triaxiality or triaxial stress and Lode angle, respectively; both are stress-dependent parameters. This criterion mode uses the graph  $\eta$  versus  $\bar{\epsilon}_f$  to describe the failure limits of a given material and is called the fracture envelope. Mathematical models are determined to obtain an equation that can provide the plastic deformation in the fracture based on the stresses applied to the specimen. Habibi et al. [5] used five mathematical models of the ductile damage model; they are Modified Mohr Coulomb [6], Maximum Shear Stress [7], Johnson and Cook [8], Lou et al. [9], and Oh and Chen [10]. All these mathematical models are showed below.

Modified Mohr Coulomb (MMC):

$$\bar{\epsilon}_f = \left\{ \frac{A}{C_2} \left[ C_3 + \frac{\sqrt{3}}{2-\sqrt{3}}(1-C_3) \left( \sqrt{\frac{3+\mu^2}{3}} - 1 \right) \right] X \left[ \sqrt{\frac{1-C_1^2}{3+\mu^2}} + C_1 \left( \eta + \frac{1}{3} \left( \frac{\mu}{\sqrt{3+\mu^2}} \right) \right) \right] \right\}^{-\frac{1}{n}} \quad (2)$$

Maximum Shear Stress (MSS):

$$\bar{\epsilon}_f = \left\{ \frac{A}{C_2 \sqrt{3 + \mu^2}} \right\}^{-\frac{1}{n}} \quad (3)$$

Johnson-Cook:

$$\bar{\epsilon}_f = C_1 + C_2 e^{(-C_3 \eta)} \quad (4)$$

Lou and Huh:

$$\bar{\epsilon}_f = C_1 \left( \frac{2}{3\sqrt{3 + \mu^2}} \right)^{-C_2} \left( \frac{1 + 3\eta}{2} \right)^{-C_3} \quad (5)$$

Oh et al.:

$$\bar{\epsilon}_f = C_1 \left\{ \eta + \frac{3 - \mu}{3\sqrt{3 + \mu^2}} \right\}^{-1} \quad (6)$$

The constants  $C_1, C_2$ , and  $C_3$  are obtained through practical tests [3]. The number of constants in each model indicates the number of tests required to determine the complete mathematical model. The main need for the experiments is to know the exact triaxiality of each test. The variable  $\mu$  is called the Lode parameter. The triaxiality value is described in Eq. (7).

$$\eta = -\frac{p}{q} \quad (7)$$

where

$$p = -\frac{1}{3}(\sigma_1 + \sigma_2 + \sigma_3) \quad (8)$$

$$q = \sqrt{\frac{1}{2}[(\sigma_1 - \sigma_2)^2 + (\sigma_2 - \sigma_3)^2 + (\sigma_3 - \sigma_1)^2]} \quad (9)$$

The term  $p$  Eq. (8) is the hydrostatic pressure and  $q$  Eq. (9) is the Von Mises stress or equivalent stress. Both are expressed in terms of stresses in the principal directions ( $\sigma_1, \sigma_2$ , and  $\sigma_3$ ). For uniaxial tensile test, the value of  $\eta$  is 0.33 since  $\sigma_2 = \sigma_3 = 0$ . For pure compression test, the value of  $\eta$  is  $-0.33$  since the same stress state from tensile test is obtained but  $\sigma_1$  acting in the opposite direction. For values that simulate another stress state, it is necessary to change the specimen geometry to obtain a known triaxial

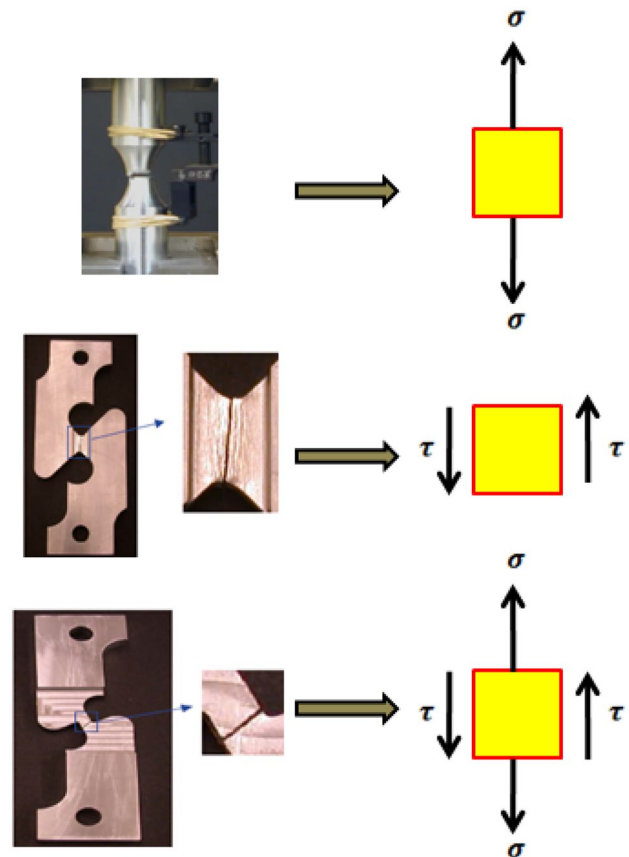


Fig. 1 Specimens used by [3] to define the fracture envelope

stress state [3, 11]. Figure 1 shows some specimens used by [3] to plot the curve  $\eta$  versus  $\bar{\epsilon}_f$ .

The purpose of the work is to find an initial estimation of formability measured by punch depth which can be implemented by a quick input during the development of a new stamping geometry. This initial estimation is obtained by using different failure criteria on FEA simulation instead of practical tests that are usually required to measure forming limits.

## 1.1 Materials and methods

The computational code was developed in a commercial version of ABAQUS software which was fed with data from the DP600 steel. The results of the present work were compared to the results obtained with the experimental data presented in the study [12], where the formability of the DP600 steel with the variation of the blank holder load (BHL) was previously evaluated. To prove the model validity, the configurations of the blank, die, BHL, and the punch were defined in order to get closer to the parameters used by [12]. The Nakazima tool geometry used in the practical tests and in the computational model is shown in Fig. 2.

The blank holder, die, and punch were modeled as solid shell elements since their deformation is not evaluated during the analysis. The sheet was modeled as deformable shell due to purpose of evaluating its deformation during the process. Shell elements being less stiff capture the mode shapes

accurately and with a fewer number of nodes and elements. This makes the analysis faster. The shell element type for the sheet was S4R (4-node general-purpose shell with reduced integration) integration type. The model was divided in three parts. The 1<sup>st</sup> part was the contact between blank holder and die, the 2<sup>nd</sup> part is the blank holder force application, and the 3<sup>rd</sup> part was the vertical motion from the punch pushing the sheet downwards through the die. For this model, it was used the penalty contact method.

The failure criterion used in the work was approximated for the plane stress state and its approach is also interesting for the sheet modeling in the shell format. The shell format will not consider the analysis of stress and deformation in the direction of the sheet thickness [13]. Figure 3 summarizes the formats and types defined for the simulations.

The finite element simulation was done in three steps: 1st step—contact between the blank holder and the blank; 2nd step—application of the BHL load; and the 3rd step—vertical displacement of the punch. The default value of the time period in ABAQUS application was 1, i.e., the time varies from 0.0 to 1.0 throughout the simulation step. The time increments in each analysis are simply fractions of the total period of each simulation step [13]. In this study, the punch displacement step time is  $10 \times$  longer than the time of the 1st and 2nd steps. For the computational simulations, the same BLF levels used by [12], in his practical tests, were defined for the present study. In this case, three BLF loads were used: 58, 80, and 130 tons.

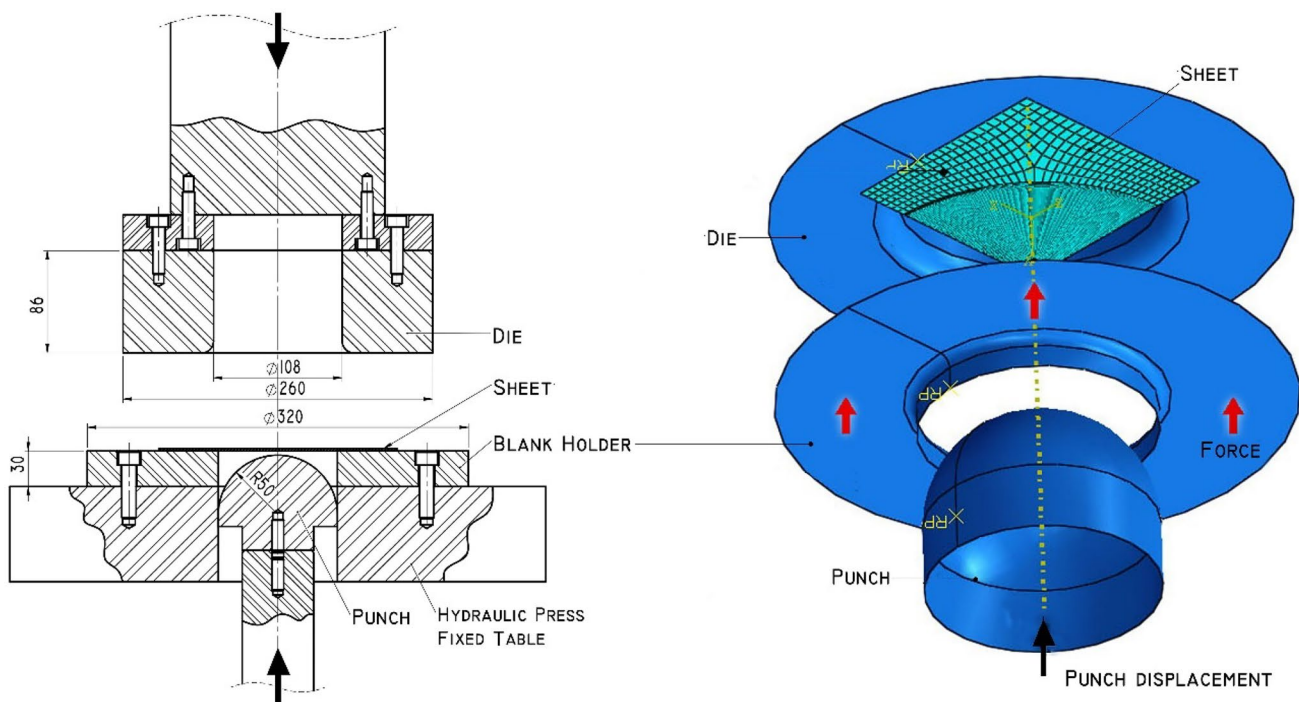
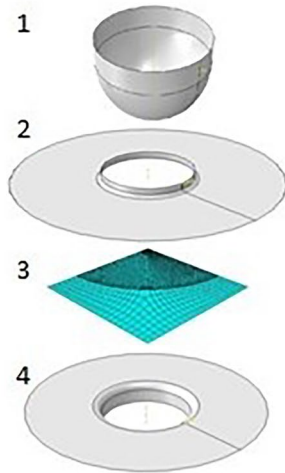


Fig. 2 Drawing of the modified Nakazima tool used for tests and the computational model

**Fig. 3** Computational model and its characteristics



Sequence	Name	Format	Type
1	Punch	Shell	Rigid
2	Blank holder	Shell	Rigid
3	Sheet	Shell	Deformable
4	Die	Shell	Rigid

It is important to clarify the conditions under which the failure criteria are reached in the ABAQUS models defined in this work. Abaqus software automatically erases the elements at the crack location. It was selected an increment of 0.1 mm from punch displacement to extract the exact punch displacement when the crack initiates.

To define the fracture envelopes of Eqs. (2), (3), (4), (5) and (6), it was necessary to leave all terms on the right side of the equation as a function of  $\eta$ . This allows to vary the value of  $\eta$  with an increment value and observe the corresponding value of  $\bar{\epsilon}_f$  for each value of  $\eta$ . In this way, it is possible to obtain the trace of the fracture envelope curve. According to [2] for the plane strain state, the Lode angle can be related to triaxiality through Eq. (10):

$$-\frac{27}{2}\eta\left(\eta^2 - \frac{1}{3}\right) = \sin\left(\frac{\bar{\theta}\pi}{2}\right) \tag{10}$$

The Lode angle and the Lode parameter are related by Eq. (11).

$$\tan(\bar{\theta}) = \frac{\sqrt{3}(1 + \mu)}{3 - \mu} \tag{11}$$

Using Eqs. (10) and (11) to leave Eqs. (2), (3), (4), (5) and (6) in function only of triaxiality, we obtain the equations below:

Modified Mohr Coulomb:

$$\bar{\epsilon}_f = \left\{ \frac{A_3 f_3}{C_2} \left[ \sqrt{\frac{1 + C_1^2}{3}} f_1 + C_1 \left( \eta + \frac{f_2}{3} \right) \right] \right\}^{-\frac{1}{n}} \tag{12}$$

Maximum Shear Stress:

$$\bar{\epsilon}_f = \left\{ \frac{A_3 f_1}{C_2 \sqrt{3}} \right\}^{-\frac{1}{n}} \tag{13}$$

Johnson-Cook:

$$\bar{\epsilon}_f = C_1 + C_2 e^{(-C_3 \eta)} \tag{14}$$

Lou and Huh:

$$\bar{\epsilon}_f = C_1 \left( \frac{2\sqrt{3}}{9} f_1 \right)^{-C_2} \left( \frac{1 + 3\eta}{2} \right)^{-C_3} \tag{15}$$

Oh et al.:

$$\bar{\epsilon}_f = C_1 \left( \eta + \frac{f_1}{\sqrt{3}} + \frac{f_2}{3} \right)^{-1} \tag{16}$$

The values of  $f_1$ ,  $f_2$ , and  $f_3$  are called simplifying functions and they can be obtained according to Eqs. (17), (18) and (19) [14].

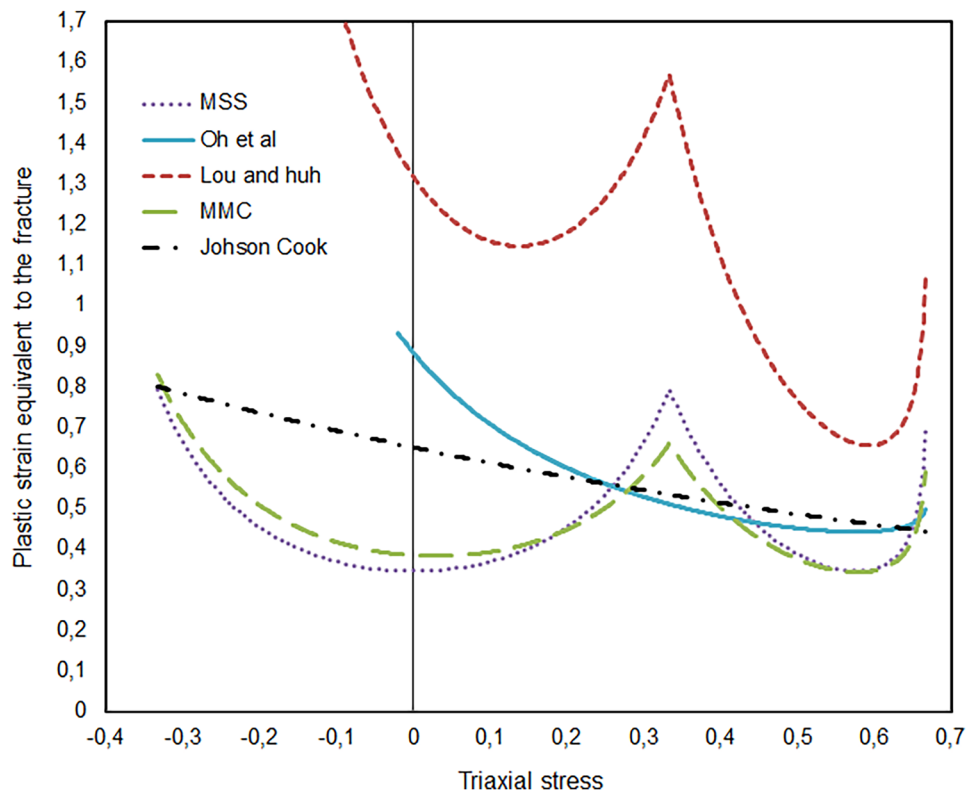
$$f_1 = \cos\left\{ \frac{1}{3} \sin^{-1} \left[ -\frac{27}{2} \eta \left( \eta^2 - \frac{1}{3} \right) \right] \right\} \tag{17}$$

$$f_2 = \sin\left\{ \frac{1}{3} \sin^{-1} \left[ -\frac{27}{2} \eta \left( \eta^2 - \frac{1}{3} \right) \right] \right\} \tag{18}$$

$$f_3 = C_3 + \frac{\sqrt{3}}{(2 - \sqrt{3})} (1 - C_3) \left( \frac{1}{f_1} - 1 \right) \tag{19}$$

Using the calibration constants obtained by [1] for the DP600 steel, the five fracture envelopes in Fig. 4 were obtained. The curve data were useful to feed the ABAQUS

**Fig. 4** Fracture envelopes obtained with the constants determined by [5] for the DP600



software as a failure criterion. Pure tensile test, pure compression or pure shear tests are used to calculate the constants, Fig. 1.

The shape of the curve from Fig. 4 is explained by the behavior from the ductile damage equation for each

criterion. Johnson-Cook has an exponential equation while Oh et al. has a linear equation. Criteria with similar curve shapes were not selected to use since Oh et al., for example, presented minor errors when compared to other criteria as illustrated by Fig. 7.

**Fig. 5** Fundamental mechanical properties and true stress vs true strain curve obtained by [15]

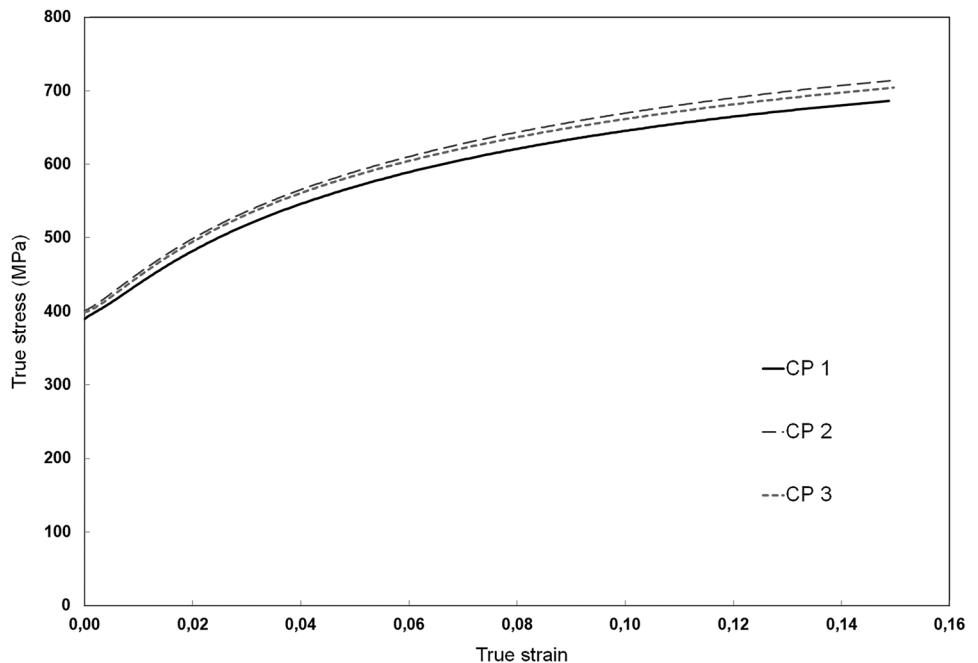
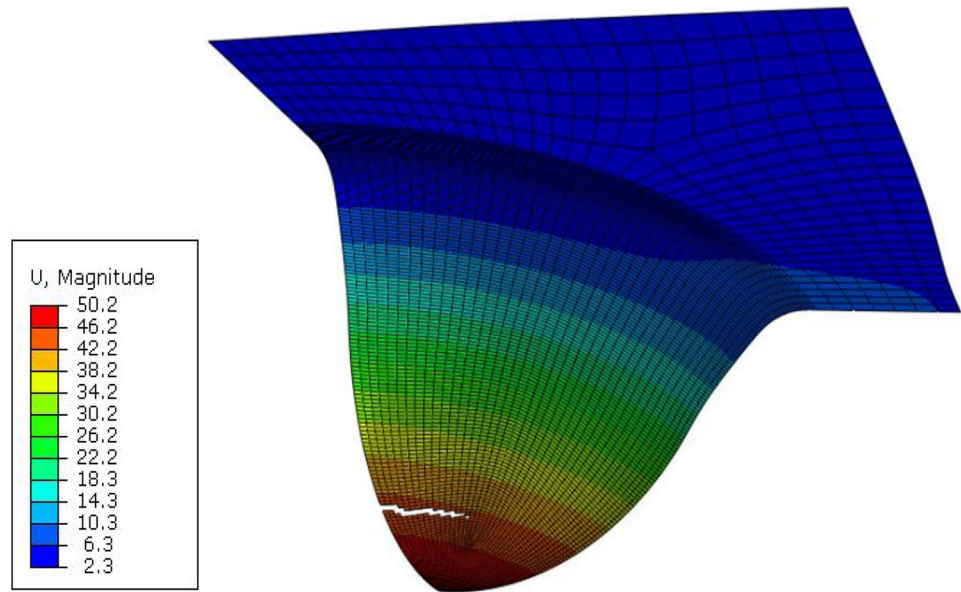


**Fig. 6** Crack initiation by failure criteria implemented in the computational model



The values of  $\epsilon_1$  and  $\epsilon_2$  (major and minor true strains) were also obtained by [12] via the Nakazima test of DP600. These values were used to implement the FLC criteria in the computational model. The fundamental mechanical properties and true stress-by-true strain curve for DP600 steel obtained by [15], as illustrated in Fig. 5, were also used.

## 2 Results

The stamping depth was the compared variable among the failure criteria (total punch displacement at the exact fracture point). Figure 6 demonstrates the exact moment when the fracture occurs in the blank. For the three BHL (58, 80, and 130 tons), the errors were calculated in relation to the practical values obtained from the punch force vs displacement curves. Chemin [12] recorded the beginning of the crack by means of pressure drop sensors in the punch, and a computer system that recorded values of force and displacement. The values of the stamping depth to the beginning of the crack were compared with the value obtained through computer simulation. Figure 6 illustrates a crack initiation in the sheet during the computational

model execution considering a failure criteria inserted in the material characterization.

The stamping depths obtained at the crack starting are summarized in Table 1.

The computational results for the BHL of 58 tons showed very good convergence with the practical results obtained by [12], for the FLC criterion, and with a good convergence for the Lou and Huh criterion, which is illustrated in Fig. 7a.

For the BHL of 80 tons, the criteria that shown nearest results to [12] were the FLC and the Modified Mohr–Coulomb (MMC), as can be seen in Fig. 7b. The MMC fracture model was derived by [14] from the original Mohr–Coulomb criterion, by transforming it from the stress space to the mixed stress–strain space, and thus formulating the equivalent plastic strain to fracture  $\bar{\epsilon}_f$ , as a function of  $\eta$  and  $\theta$ . It takes the form of an equation that led to Eq. (1) and so the models are similar.

The errors obtained for the simulation with the BHL of 130 tons are shown in Fig. 7c. The results for Johnson–Cook, Maximum Shear Stress (MSS), and Oh et al. were the ones that came closer to the results obtained by [12] because the models assume that the equivalent plastic strain at the onset of damage is a function of stress triaxiality and strain rate.

**Table 1** Stamping depths (in mm) obtained in the tests

Failure criterion	Johson-Cook	Lou and Huh	MMC	MSS	Oh et al	FLD	Chemin Filho (2011)
58 tons	45.6	58.5	47.4	45.3	48.3	54	53.6
80 tons	42.6	54.6	45.6	43.8	44.7	50.1	48
130 tons	39.2	51	42.6	40.8	40.8	46.2	39.6

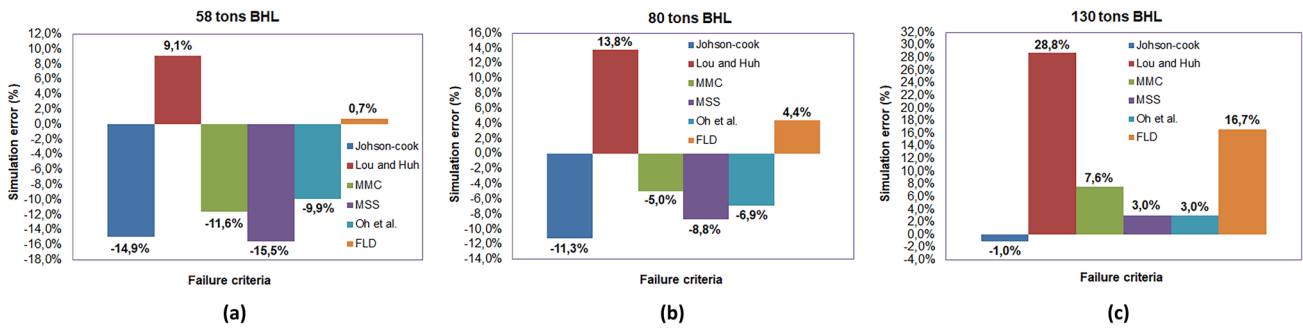


Fig. 7 Errors obtained by computational models for a BHL of 58 tons a, 80 tons b, and 130 tons c

It was observed that Lou and Huh and the FLC criteria showed larger errors when the sheet restriction is not so expressive. That is, when the sheet is under little restraint (low BHL strength), the simulation result of the Lou and Huh model is closer to the experimental one, with an error of only 9%. However, the model greatly increases the error when higher HLB loads are applied and leads to stretching. The same meshing was applied for all the simulations and if the mesh is reduced all the results could be changed by the same amount proportionally. It was used a mesh of  $0.5 \times 0.5$  elements at a circular section of 50-mm radius and  $2 \times 2$  elements at the remaining sheet, Fig. 8.

Most of the maximum punch depth values obtained for the computationally simulated failure criteria showed a linear trend or very close to linear. On the other hand, the results obtained by [12] deviate from the trend obtained by the computational results, see Fig. 9. The computational deviation can be justified by disconsider the changes in the elasticity modulus during the plastic deformation of the sheet and Bauschinger effect.

The experimental result obtained by [12] shows that the result is not linear and some models that do not present this behavior may present some limitations of mathematical description. However, the proposed FLD model was

Fig. 8 Meshing applied for all the simulations

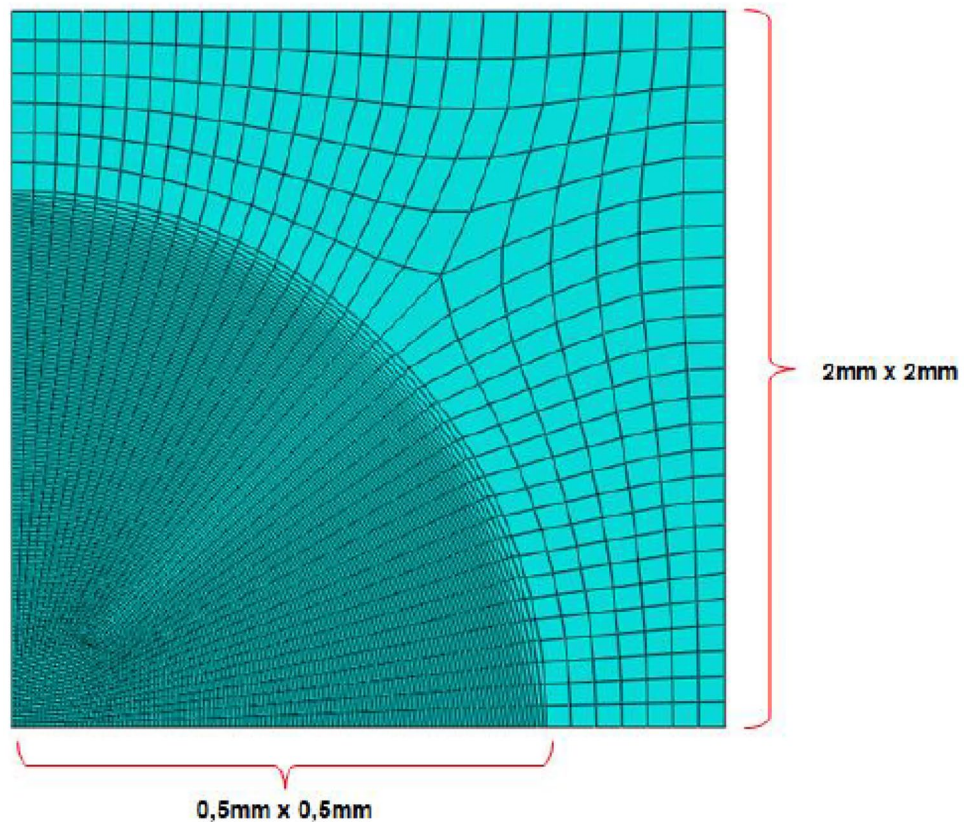
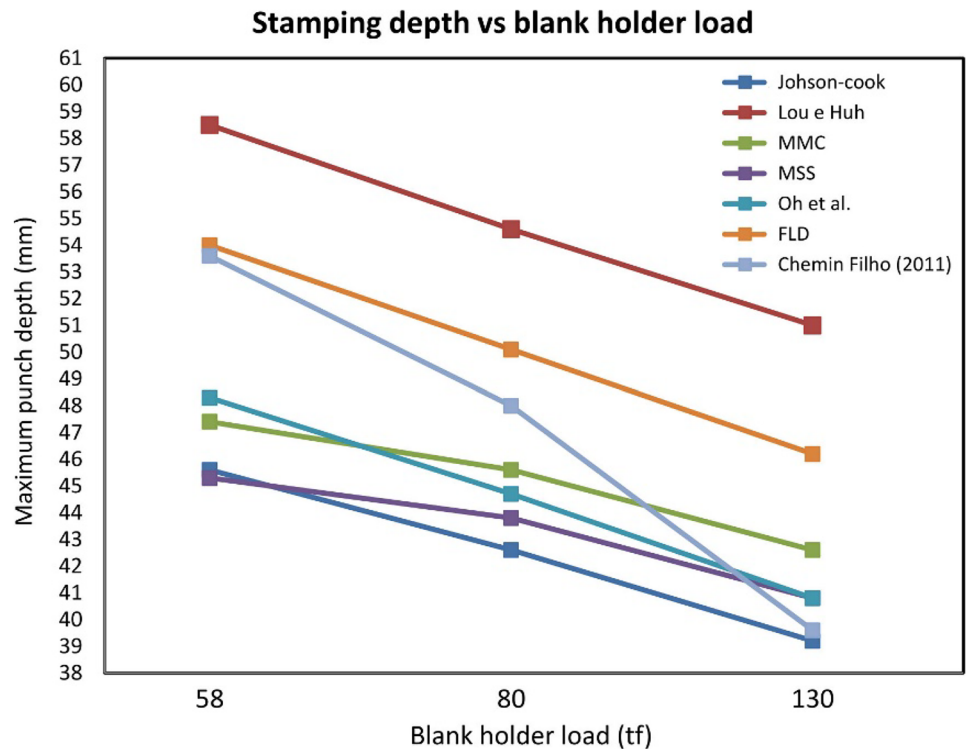


**Fig. 9** Comparison between the obtained results



able to predict very closely the crack initiation depth for the BHL of 58tf and 80tf (deep drawing) without the need for complex conformability tests, only with simple tensile tests.

The failure criteria obtained by FEA did not achieve a greater result accuracy when compared to the failure criteria obtained by the Nakazima test [12]. For the elaboration of the FLC failure criteria, a sequence of tests with controlled conditions and parameters is required, which makes difficult the obtention of all the data. Some of the failure criteria of the ductile damage model require only one uniaxial tensile test for its determination, which becomes interesting when compared to the FLC criteria.

It was observed that for each blank holder load, there was a criterion that was closer to the results obtained by [12]; such behavior can be studied for the selection of the rupture criterion to be used in a given or specific application. For example, in addition to the FLC criterion, Lou and Huh criterion obtained a reasonable simulation error for loads of 58 tons while the Johnson-Cook criterion resulted in a 1% error for 130 tons.

As seen in Fig. 7, in the cases with a small amount of sheet restriction, an approximation with 6% error was obtained for the Oh et al. criterion when compared to the result reproduced by [12] for blank holder load of 58 tons. The FLC criterion distanced itself from the results obtained by [12] in cases with greater sheet restriction, while the MSS criterion raised with the data of [16] resulted in an error

of 7.1% for the blank holder load of 130 tons. Such errors become interesting since the determination of the Oh et al. and MSS criteria require only one tensile test.

The approximations obtained by the Habibi et al. criteria [5] diverged from the results of [12] due to the fact that the DP600 steel used in the tests to determine the calibration constants did not have the same characteristics (composition and mechanical properties) of the steel used by [12].

### 3 Conclusion

The results for the failure criteria numerically obtained with ABAQUS software did not reach a good precision if compared to the results obtained by the FLC.

In summary, the following factors can be highlighted from the performed experiments:

- Linear behavior of the stamping depths obtained by the computational tests was observed while the same trend was not observed for the experiments performed by [12]—further study of the fracture mechanism of DP or AHSS steels becomes necessary;
- Some criteria showed lower errors at specific blank holder loads, such result can be used for a practical implementation having the sheet restriction intensity as a selection criterion for the rupture criterion;

- Criteria where only one uniaxial tensile test is needed for model calibration, showed errors in the range of 3–7%. This fact becomes interesting when compared to the determination of a failure criterion by Nakazima test or via three practical tests according to some criteria of the ductile damage model.

In this study, for each blank holder load (BHL) applied to the stamped sheet, at least one failure criterion presented more convergence to the results obtained by [12]. Such behavior can be studied for the selection of the failure criterion to be applied in a given application. For example, in addition to the FLC criterion, Lou and Huh criterion showed a reasonable simulation error for the BHL of 58 tons while the Johnson–Cook criterion resulted in a 1% error for the BHL of 130 tons. Thus, in the case where the sheet metal is in a very restricted condition it becomes feasible to use the Johnson–Cook criterion.

Is very important to note that is more interesting to use a failure criterion with only one calibration constant, as the case of the Maximum Shear Stress (MSS) and the Oh et al. criterion. Such criteria were able to deliver a computational error of 3% for the BHL of 130 tons and an average error of 7% for the BHL of 80 tons. As the most striking contribution is worth to note that the two criteria mentioned above can be obtained by a simple uniaxial tensile test.

For the sheet metal industry, the present work can help in the try-out operations and the tooling development or modification. Numerical simulations using specific failure criterion are useful tool to have a first approach of the forming process parameters to be implemented during the try-out of new product. Also, the failure criteria simulations can be used to troubleshoot stamping issues based on strain analysis and sheet formability.

**Funding** Mr. Paulo Victor Prestes Marcondes received grant from CNPq Agency (Brazil).

## Declarations

**Ethics approval** Not applicable.

**Consent to participate** Not applicable.

**Consent for publication** The authors consent for the publication of the present work.

**Conflict of interest** Not applicable.

## References

1. Keeler S, Menachem K (2014) Advanced high-strength steels application guidelines. Worldautosteel
2. Tepedino JA (2014) Aplicação de Curvas Limite de Conformação na previsão de rupturas em bordas de peças estampadas
3. Bao Y, Wierzbicki T (2004) On fracture locus in the equivalent strain and stress triaxility space. *Int J Mech Sci* 46(1):81–98
4. Wierzbicki T, Bao Y, Lee Y-W, Bai Y (2005) Calibration and evaluation of seven fracture models. *Int J Mech Sci* 47:719–743
5. Habibi N, Ramazani A, Prah U (2017) Failure predictions of DP600 steel sheets using various uncoupled fracture criteria. *Eng Fract Mech* 1–15
6. Dunand M, Mohr D (2000) Determination of (multiaxial) ductile fracture properties of trip steel sheets using notched tensile specimens. Report 193. Technical report, Impact and Crasworthiness Laboratory. MIT, Cambridge, MA
7. Tresca H (1864) Memoir on the flow of solid bodies under strong pressure. *Comptes-rendus de l'académie des sciences* 59:754–8
8. Johnson GR, Cook WH (1985) Fracture characteristics of three metals subjected to various strains, strain rates, temperatures and pressures. *Eng Fract Mech* 101:36–44
9. Lou Y, Huh H, Lim S, Pack K (2012) New ductile fracture criterion for prediction of fracture forming limit diagrams of sheet metals. *Int J Solids Struct* 49:3605–3615
10. Oh S, Chen C (1979) Kobayashi S. Ductile fracture in axisymmetric extrusion and drawing - part 2: workability in extrusion and drawing. *J Eng Industry* 101:36–44
11. Pack K, Luo M, Wierzbicki T (2014) Sandia Fracture Challenge: blind prediction and full calibration to enhance fracture predictability. *Int J Fract* 186:155–175
12. Chemin Filho RA (2011) Estudo da fratura de aços de nova geração DP600 através da variação de pressão no prensa-chapas. Tese de Doutorado em Engenharia Mecânica pela Universidade Federal do Paraná
13. Abaqus (2014) V16.4/CAE - User's Guide
14. Bai Y, Wierzbicki T (2010) Application of extended Mohr–Coulomb criterion to ductile fracture. *Int J Fract* 161(1):1–20
15. Lajarin SF, Marcondes PVP (2018) Dependence of plastic strain and microstructure on elastic modulus reduction in advanced high-strength steels. *J Braz Soc Mech Sci Eng* 40:87
16. Lajarin SF (2012) Influência da variação do módulo de elasticidade na previsão computacional do retorno elástico em aços avançados de alta resistência. Tese de Doutorado em Engenharia Mecânica pela Universidade Federal do Paraná

**Publisher's Note** Springer Nature remains neutral with regard to jurisdictional claims in published maps and institutional affiliations.